

# Luminous Matter Distribution, Bulk Flows and Baryon Content in Cosmological Models with a Local Void

Kenji TOMITA\*

*Yukawa Institute for Theoretical Physics, Kyoto University,  
Kyoto 606-8502, Japan*

(Received February 27, 2002 )

First, we consider galaxy formation from the viewpoint of hierarchical clustering theory and discuss the possibility that inhomogeneous models with a local void may be compatible with the observed homogeneity of galactic distributions found in recent redshift surveys, because their inhomogeneity can be weakened by the difference in the feedback system of galaxy formation between the inner and outer regions. Next, it is shown with the results of numerical simulations that the observed inhomogeneity of two-point correlations of galaxies can be accounted for by these models. Also, the natural appearance of bulk flows for an off-central observer is demonstrated. Finally, the inhomogeneity of the baryon content is discussed from the viewpoint of our inhomogeneous models.

## §1. Introduction

Under the assumption of spatial homogeneity, cosmological parameters have been determined using important observational results, such as the [magnitude  $m$  - redshift  $z$ ] relation of type Ia SN<sup>1), 2), 3), 4)</sup> and the anisotropy of cosmic microwave background radiation (CMB),<sup>5), 6), 7), 8), 9)</sup> and it has been found that models with a dominant cosmological constant best describe the SN data and flat models best describe the CMB data.

The present author<sup>10)</sup> has considered models with a local void on scales of  $\sim 200$  Mpc in order to explain the existence of the large-scale bulk flows measured by Hudson et al.<sup>11)</sup> and Willick,<sup>12)</sup> and has shown<sup>13), 14), 15)</sup> that the zero  $\Lambda$  and small  $\Lambda$  models with flat space in the outer region are consistent with the data of type Ia supernovae (especially the recent data for  $z = 1.7$ <sup>16)</sup>) and with the CMB anisotropy. It thus appears that these models are competent for accounting for the cosmological observations in spite of the small realization probability of their large-scale void. Here the void means a low-density region with respect to the total matter, which consists mainly of the dark matter.

The homogeneity of galactic distributions found in recent redshift surveys may support homogeneous models, but it does not necessarily rule out the inhomogeneous models with a local void, in which the galactic number densities in the inner and outer regions may be comparable owing to a larger suppression of galaxy formation in the outer region.

In this paper we consider in §2 the process of galaxy formation and observational aspects of inhomogeneous models from the viewpoint of hierarchical galaxy

---

\* E-mail address: tomita@yukawa.kyoto-u.ac.jp

formation theories. To demonstrate the feasibility of the inhomogeneous models, it is necessary to show how they can predict a nearly homogeneous distribution of galaxies in spite of their void structure. Here we study the observed galactic distributions in connection with the existence of a local void and the two-point correlation that reflects gravitationally the inhomogeneous structure of our models. In §3, we describe the models with a local void using numerical simulations, and in §4, we analyze the theoretical two-point correlations ( $\xi^I$  and  $\xi^{II}$ ) in the inner and outer regions and show that the computed ratio  $\xi^I/\xi^{II}$  is consistent with the observed ratio. In §5, we derive the bulk flows for an off-center observer. In §6 we discuss the inhomogeneity of the baryon content from the point of view provided by our models. Section 7 is dedicated to concluding remarks.

## §2. Galaxy formation and observational aspects

Modern theories of galaxy formation led to a great deal of progress in the understanding of galactic properties under the assumption of cold dark matter (CDM) in hierarchical clustering cosmologies. In these models, it is assumed that galaxies form when gas cools and condenses in dark matter halos that merge during their evolution. The key point in these theories is that the energy released from stars acts as a “negative feedback” on the gas and star formation. This idea was proposed by White and Rees<sup>17)</sup> and developed by White and Frenk.<sup>18)</sup>

Recent works on galaxy formation, including the process of feedback, have employed two important methods, a semi-analytic method and numerical simulations. The first is directly connected with the above two pioneering works and takes into account the feedback in detail, but has been applied only in simplified (spherically symmetric) situations. The merger history of a dark matter halo has been treated using either a statistical method (Kauffmann et al.,<sup>19)</sup> Cole et al.,<sup>20), 21)</sup> Somerville and Primack<sup>22)</sup>) or with  $N$ -body simulations (Kauffmann, Nusser and Steinmetz,<sup>23)</sup> Kauffmann, Colberg, Diaferio and White,<sup>24)</sup> Benson et al.,<sup>25)</sup> Somerville et al.<sup>26)</sup>). In the case of simulations, both the merger history (using  $N$ -body simulations) and the feedback process and star formation (using gas dynamical simulations) have been investigated (Cen and Ostriker,<sup>27)</sup> Katz, Weinberg and Hernquist,<sup>28)</sup> Frenk et al.,<sup>29)</sup> Kay et al.<sup>30)</sup>). This method has the advantage that no artificial symmetries need to be imposed, but it has the disadvantage that the treatment is not transparent and there are unrealistic limits on the dynamic range of resolved structures, though the resolution is being improved with the use of high-speed supercomputers. In the following, we first give an outline of recent treatments of galaxy formation on the basis of the semi-analytic method of Kauffmann et al., and next consider how we should treat galaxy formation in the present models with a local void.

### 2.1. Galaxy formation in homogeneous models

The semi-analytic models of Kauffmann et al.<sup>24)</sup> consist of a combination of  $N$ -body simulations and an analytic approach to star formation and supernova feedback. The  $N$ -body simulations are performed using the cluster normalization by determining  $\sigma_8$ , the dispersion of density perturbations, within  $8h^{-1}$  Mpc spheres in

two CDM models: SCDM ( $\tau$ model) and  $\Lambda$ CDM, with

$$(\Omega_0, \lambda_0, h, \sigma_8, \Gamma, f_b) = (1.0, 0.0, 0.5, 0.6, 0.21, 0.1), \quad (0.3, 0.7, 0.7, 0.7, 0.9, 0.21, 0.15),$$

respectively, where  $\Gamma$  is the shape parameter of the power spectrum and  $f_b$  is the baryon factor ( $\equiv \Omega_b/\Omega_0$ ).

The merging history of dark matter halos is constructed using the halo catalogues that consist of halos larger than the least stable system (containing 10 particles). In each halo, there is a central particle, representing the central galaxy onto which gas in a halo falls and where stars form. The central galaxy in a halo is the central galaxy in its most massive progenitor, and the central galaxies in less massive progenitors are satellites in the halo. These galaxies also grow from small galaxies to larger galaxies through merging.

The physical properties of galaxies are determined by gas cooling, star formation, supernova feedback, dust extinction, etc. The most important processes among them are star formation and supernova feedback. Here, a star formation rate of the form

$$dM_*/dt \ (\equiv \dot{M}_*) = \alpha M_{\text{cold}}/t_{\text{dyn}} \quad (2.1)$$

is assumed, where  $\alpha$  is a free parameter,  $t_{\text{dyn}}$  is the dynamical time of the galaxy, and  $M_*$  and  $M_{\text{cold}}$  are the total masses of stars and cold gas in the halo, respectively.

The energy ejected by a supernova explosion into the interstellar medium reheats the cold gas to the virial temperature. The reheating rate is expressed as

$$dM_{\text{reheat}}/dt = \epsilon \frac{4}{3} \dot{M}_* \eta_{\text{sn}} E_{\text{sn}}/V_c^2, \quad (2.2)$$

where  $\eta_{\text{sn}}$  is the number of supernovae per solar mass of stars ( $= 5 \times 10^{-3}/M_\odot$ ),  $E_{\text{sn}}$  is the kinetic energy of the ejection from each supernova ( $\cong 10^{51}$  erg),  $\epsilon$  is a free parameter representing the fraction of this energy used to reheat cold gas, and  $V_c$  is the circular velocity of galaxies.

The evolution of distributions of dark matter halos and galaxies within them is determined using Eqs. (2.1) and (2.2), when we specify the free parameters  $\alpha$  and  $\epsilon$ , and the present distributions can be compared with observations in the form of luminosity functions, Tully-Fisher relations and two-point correlations. In order to choose the best values of  $\alpha$  and  $\epsilon$ , a normalization condition is imposed: a fiducial reference galaxy (which is defined as a central galaxy with  $V_c = 220 \text{ km s}^{-1}$ ) is assumed to satisfy the *I*-band Tully-Fisher relation. Then the set  $(\alpha, \epsilon)$  is given as (0.07, 0.15) and (0.1, 0.03) for the SCDM ( $\tau$ CDM) and  $\Lambda$ CDM models, respectively. These values imply that the SCDM model has smaller star formation and larger feedback than the  $\Lambda$ CDM model. For these sets, both the SCDM and  $\Lambda$ CDM models have luminosity functions, Tully-Fisher relations and two-point correlations consistent with the observed ones. In addition to the feedback due to supernova explosions, photoionization and heating due to ultraviolet radiation also contribute to the feedback. <sup>31), 32), 33)</sup>

## 2.2. Galaxy formation in models with a local void

In these models the total matter (consisting mainly of dark matter) has different uniform densities in the inner region ( $r < r_b$ ) and the outer region ( $r > r_b$ ), and, sim-

ilarly the luminous matter (consisting of galaxies) may also have different densities in the two regions. If the star formation and the feedback effect in the two regions act in a cooperative manner, however, the distributions of the luminous matter can be nearly uniform throughout the two regions.

Let us assume for instance that the outer region is represented by the Einstein-de Sitter model and the inner region is represented by an open model with  $(\Omega_0, \lambda_0) = (0.3, 0)$ . Then we can have  $(0.07, 0.15)$  as the set  $(\alpha, \epsilon)$  in the outer region. Because the model in the inner region is similar to the low-density model with  $(\Omega_0, \lambda_0) = (0.3, 0.7)$ , we have  $(\alpha, \epsilon) \approx (0.1, 0.03)$  in the central part of the inner region, say  $r \leq r_{\text{in}} (\leq r_b)$ .

In the transient region satisfying  $r_{\text{in}} \leq r \leq r_b$ , the values of the set  $(\alpha, \epsilon)$  change gradually from the value  $(0.07, 0.15)$  in the outer region to the value  $(0.1, 0.03)$  in the inner region. The strong photoionization by UV radiation from the outer region to the inner region may play an effective role in preventing small galaxies from forming and hence growing through merging in this region. For this reason, the number density of forming galaxies is small there, compared with the densities in the outer and inner regions.

Galaxies formed in the transient region enter the outer region thereafter, colliding with other galaxies there, since the inner expanding velocities are larger than the outer velocities. At the present epoch, the boundary ( $r = r_{\text{in}}$ ) of the inner central region reaches the boundary  $r = r_b$  of the outer region, so that the number densities of galaxies in the outer and inner regions may be nearly equal, as shown in Fig. 1. At present, however, we cannot determine the position  $r = r_{\text{in}}$  accurately, since studies on the dependence of rates of star formation, supernova explosion and UV radiation on the background models have not yet been established.<sup>34)</sup> Depending on these rates and the position of the central part ( $r < r_{\text{in}}$ ), the various large-scale structures may appear around the boundary ( $r = r_b$ ). It is found in simple simulations that, if radial distances for  $r_{\text{in}} \leq r \leq r_b$  are about 1/4 of those satisfying  $0 \leq r \leq r_b$  on the comoving scale, the two regions become smoothly connected later.

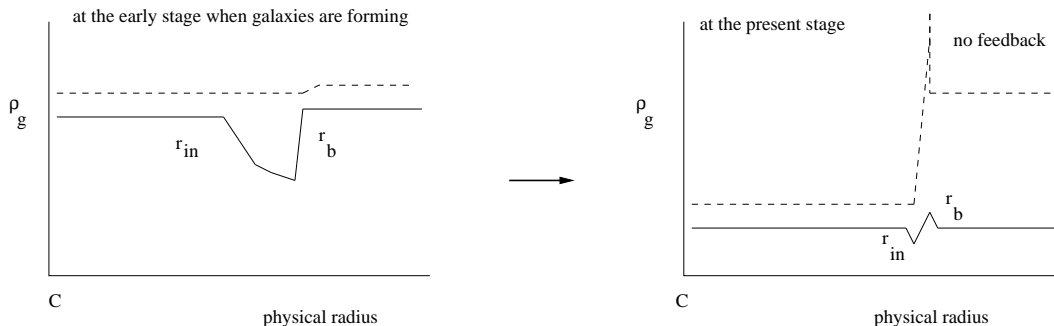


Fig. 1. The schematic evolution of galactic density  $\rho_g$  around the boundary  $r_b$ . The dashed curves correspond to the case of no feedback.

Here we have the important prediction that around the boundary there must be many active galaxies that are born as a result of the frequent collisions of galaxies, even if the distribution of galaxies is smooth there owing to strong feedback.

It is important to investigate the evolution of luminous matter using numerical simulations, taking into account the above described complicated processes including cooling, star formation, supernova feedback and heating by UV radiation, but such investigations are far beyond the scope of this paper. At present, we cannot show quantitatively how luminous matter becomes nearly homogeneous, but we are able to describe a possible process leading to the approximate homogeneity.

### 2.3. Observed galactic distributions

Here we consider the present observational situation regarding the galactic distribution from the viewpoint of our inhomogeneous models.

#### 2.3.1. Dependence on the observer's position

Several redshift surveys have suggested the existence of a low density region or a local void with radius  $\sim 300h$  Mpc ( $H_0 = 100h$  km sec $^{-1}$  Mpc $^{-1}$ ).<sup>35), 36), 37), 38)</sup> The latest surveys (2dF and SDSS) show that the galactic distributions within a radius  $\sim 600h$  Mpc are homogeneous on the whole, though they include various large-scale structures. Thus the observed distributions seem to be consistent with homogeneous cosmological models. However, inhomogeneous models with a local void also may be compatible with these surveys for the following reasons:

(1) The number densities of galaxies in the inner low-density region and the outer high-density region may be similar in these models also, as discussed in the previous subsection.

(2) Some of observed large-scale structures, which are regarded as independent, may represent correlated structures near the boundary. For an observer in the center, these correlated structures have an equal redshift and can easily be distinguished. For us (off-center observers), however, they have direction-dependent redshifts and can be confused with other uncorrelated structures. When we superpose the redshift histograms in various directions to the north and south, off-central observers may see the structures there as independent at different distances.

#### 2.3.2. Active galaxies around the boundary

From a recent study of spectral types of galaxies in the 2dF survey (Madgwick et al.<sup>39)</sup>), it was found that there are many active galaxies in the redshift region corresponding to the boundary  $r = r_b$ . These galaxies may have been born as a result of the above-mentioned collisions of galaxies around the boundary. Similar analyses of the spectral types of galaxies are necessary for the SDSS survey to clarify the astrophysical situation around the boundary.

#### 2.3.3. Two-point correlation

The apparent distribution of luminous matter may not be useful in the study of the background model consisting mainly of dark matter, because of the very complicated processes of formation and evolution of galaxies. The two-point correlations of galaxies, on the other hand, depend mainly on the background model, at least for less luminous galaxies in the homogeneous regions. Therefore it may be important to use these correlations to study the distribution of dark matter also.

Recently, large-scale redshift surveys have provided valuable information about

the spatial dependence of the two-point correlations of galaxies in the region  $z < 0.1$ . Using the NGP + SGP data from the 2dF surveys, Norberg et al.<sup>40)</sup> derived the correlation length  $r_0$  for samples with the various parameters ranges (cf. Table 1 and Fig. 3 in their paper). The observed correlation length increases with the absolute magnitude as  $r_0 = 4.14 \pm 0.64, 4.43 \pm 0.45, \dots, 9.38 \pm 1.48$  for  $(M_{bJ} - 5 \log_{10} h, z) = (-18.0 - -18.5, 0.010 - 0.080), (-18.5 - -19.0, 0.013 - 0.104), \dots, (-21.5 - -22.5, 0.059 - 0.28)$ , respectively, where  $M_{bJ}$  is the  $b$ -band absolute magnitude. The SSRS2, EPS and Stromlo data also exhibit a trend similar to that found in the 2dF survey, as shown in Fig. 3 in Norberg et al.'s paper.<sup>40)</sup> The luminosity dependence of  $r_0$  in these samples seems to be consistent with that discussed in the hierarchical galaxy formation theories.

According to a recent theory of galactic distribution (Benson et al.<sup>25)</sup>,  $r_0$  is an increasing function of  $-M_{bJ}$  for  $-(M_{bJ} - 5 \log_{10} h) > 21$ , while it is constant or a slightly decreasing function of  $-M_{bJ}$  for  $-(M_{bJ} - 5 \log_{10} h) < 21$ . The observed value of  $r_0$  is an increasing function of  $-M_{bJ}$  even for  $-(M_{bJ} - 5 \log_{10} h) < 21$ . Quantitatively, it increases by a factor of about 1.5 over the interval  $(M_{bJ} - 5 \log_{10} h) = -18 - -21$ . The two-point correlation  $\xi \propto r_0^\gamma$  ( $\gamma \approx 1.7$ ) changes by a factor of 2.0 over this interval. We can interpret this change to represent the redshift dependence (or the spatial inhomogeneity) of  $r_0$  or  $\xi$  in the region  $z = 0.010 - 0.280$ . The boundary ( $z \sim 0.07$ ) of the local void we consider is included in this region.

From the data of the SDSS survey, Zehavi et al.<sup>41)</sup> derived the correlation length  $r_0$  for three samples, obtaining  $r_0 = 7.42 \pm 0.33, 6.28 \pm 0.77$  and  $4.72 \pm 0.44$  for  $(M_r^*, z) = (-23.0 - -21.5, 0.100 - 0.174), (-21.5 - -20.5, 0.052 - 0.097)$ , and  $(-20.0 - -18.5, 0.027 - 0.051)$ , respectively (cf. Table 2 and Fig. 16 in their paper.) Their result also reveals a change in  $r_0$  by a factor of about 1.33 over the interval  $M_r^* = -21.5 - -18.5$ . This change can be interpreted as the redshift dependence of  $r_0$  in the interval  $z = 0.027 - 0.097$ . Our boundary ( $z \sim 0.07$ ) is also included in this interval.

In order to explain these spatial changes in  $r_0$  and  $\xi$ , we study inhomogeneous models with a local void in the following sections using simple simulations.

### §3. Numerical inhomogeneous models

In previous papers, I used models with a local void consisting of homogeneous inner and outer regions with a singular shell or an intermediate self-similar region. In order to study the evolution of nonlinear perturbations and their two-point correlations in these regions, I derived numerical inhomogeneous models using the method of  $N$ -body simulations, by considering a spherical low-density region in the background homogeneous models. These models are presented in this section. The background model parameters are expressed as  $H_0, a_0, \Omega_0$  and  $\lambda_0$ , representing the Hubble constant, the scale factor, the density parameter and the cosmological-constant parameter at the present epoch  $t = t_0$ , respectively, and the spatial curvature is  $K = a_0^2 H_0^2 (\Omega_0 + \lambda_0 - 1)$ . The proper radial distance  $R$  at  $t_0$  is related to the radial coordinate  $r$  by  $R = a_0 r$ . As the background models, we consider the following three cases:  $(\Omega_0, \lambda_0, h) =$  (1) Einstein-de Sitter model (1.0, 0.0, 0.5), (2) open model

(0.6, 0.0, 0.6) and (3) flat nonzero- $\Lambda$  model (0.6, 0.4, 0.6).

The  $N$ -body simulations were performed using the tree-code used by Suto and Sugihara, in which a periodic condition is imposed, and the initial perturbed state is determined using COSMICS. Here  $N = 2.1 \times 10^6$ , and the particle mass  $M$  is  $M = 5.7, 2.9$  and  $2.9 \times 10^{13} M_\odot$  for the above three cases (1), (2) and (3), respectively. The softening radius is 1 Mpc for all cases. The periodic condition is given at  $|x^1| = |x^2| = |x^3| = r_p$ , where  $R_p \equiv a_0 r_p = 300/h$  Mpc and  $r \equiv [(x^1)^2 + (x^2)^2 + (x^3)^2]^{1/2}$ .

The initial conditions are set at  $t = t_i$  at which  $z = z_i$  ( $= 15.5$ ), in the form of displacements  $\delta x^k$  and velocities  $v^k$  of  $N$  particles ( $k = 1, 2, 3$ ). After the initial conditions in the homogeneous case are given, a low-density region is introduced at the initial epoch by changing the particle positions  $x^k$  in the inner region ( $r < r_b$ ) and the intermediate region ( $r_b < r < r_{b1}$ ) as

$$x^k = (x^k)_{\text{hom}} \times \begin{cases} (1+d) & \text{for } r < r_b, \\ \left[ 1 + d \left( \frac{1}{r_b} - \frac{1}{r_{b1}} \right) / \left( \frac{1}{r} - \frac{1}{r_{b1}} \right) \right] & \text{for } r_b \leq r < r_{b1}, \end{cases} \quad (3.1)$$

and  $x^k = (x^k)_{\text{hom}}$  for  $r > r_{b1}$  (see Fig. 2). Here  $(x^k)_{\text{hom}}$  represents the particle positions in the homogeneous case and  $d$  is a constant expansion factor adjusted so as to give the expected density parameter and average expansion rate in the inner region. The intermediate region was introduced to make smooth the change in the density and velocity of particles near the boundary. Here, we treat mainly the case  $R_b \equiv a_0 r_b = 180/h$  Mpc and  $R_{b1} \equiv a_0 r_{b1} = 210/h$  Mpc, and consider also the case  $R_b = 120/h$  Mpc and  $R_{b1} = 140/h$  Mpc for comparison.

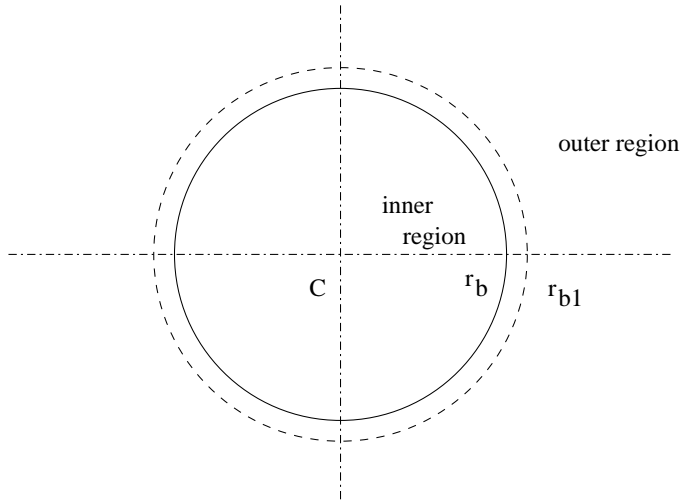


Fig. 2. Two regions and the boundary. The solid and dotted curves denote the surfaces with  $r = r_b$  and  $r = r_{b1}$ , respectively.

From the viewpoint of our models with a local void, the above model parameters describe the outer region ( $r > r_b$ ) and correspond to  $(\Omega_0^{\text{II}}, \lambda_0^{\text{II}}, h^{\text{II}})$  in the previous papers,<sup>10), 13)</sup> where  $H_0^{\text{II}} = 100h^{\text{II}} \text{ km s}^{-1} \text{ Mpc}^{-1}$ . From the simulations, the parameters  $(\Omega_0^{\text{I}}, \lambda_0^{\text{I}}, h^{\text{I}})$  in the inner region are derived as their average values in the

expression

$$H_0^I \equiv H_0^{II} + \left( \sum_{i \in I_*} v_{(i)}/r_{(i)} \right) / N_* \quad (3.2)$$

along with  $\lambda_0^I \equiv \frac{1}{3}A/(H_0^I)^2$ , where the summation is taken over the set  $I_*$  of particles included in the region  $r_l < r < r_b$  ( $r_l \sim 0.2r_b$ ), so as to avoid the disturbances near the origin and the boundary. Here,  $N_*$  is the particle number in this region, and  $v_{(i)}$  and  $r_{(i)}$  are the radial velocities and radii of the  $i$ -th particle, where  $v_{(i)} \equiv (\sum_{k=1}^3 v_{(i)}^k x_{(i)}^k) / r_{(i)}$ .

For the particles that were initially in the inner region, the observed positions (in redshift space) are different from those represented by the background coordinates (in real space). To take the average velocity (in the inner region) into account, we define other coordinates (average comoving coordinates)  $\bar{x}^k$  ( $k = 1, 2, 3$ ) as

$$\bar{x}^k = x^k \times \begin{cases} H_0^I/H_0^{II} & \text{for } r < r_b, \\ \left[ 1 + \left( \frac{H_0^I}{H_0^{II}} - 1 \right) \left( \frac{1}{r_b} - \frac{1}{r_{b1}} \right) / \left( \frac{1}{r} - \frac{1}{r_{b1}} \right) \right] & \text{for } r_b \leq r < r_{b1}, \end{cases} \quad (3.3)$$

and  $\bar{x}^k = x^k$  for  $r > r_{b1}$ . This coordinate system constitutes both an outer comoving system and an inner comoving system with respect to the mean motion. Using the volume  $V_* = \frac{4}{3}\pi a_0^3 (r_b^3 - r_l^3) (H_0^I/H_0^{II})^3$  in these coordinates, the density parameter in the inner region is defined as

$$\Omega_0^I \equiv \frac{3\pi G}{3(H_0^I)^2} \frac{MN_*}{V_*}. \quad (3.4)$$

These values in the above three cases are listed in Table I together with  $d$  and  $R_b$ . The values of  $d$  were chosen so as to obtain  $\Omega_0^I \sim 0.3$  for three sets of  $(\Omega_0^{II}, \lambda_0^{II})$ . By comparing the case  $R_b h = 180$  and the case  $R_b h = 120$ , we find that the choice of the position of the boundary is not crucial.

Table I. Inner model parameter values determined statistically for given outer model parameters  $(\Omega_0, \lambda_0, h) = (\Omega_0^{II}, \lambda_0^{II}, h^{II})$ . Here  $d$  is a constant expansion factor and  $R_b$  is the radial distance between the center C and the boundary.  $\Omega_b$  is the present baryon density parameter ( $\propto \Omega_0$ ).

$\Omega_0^{II}$	$\lambda_0^{II}$	$h^{II}$	$d$	$R_b h$ Mpc	$\Omega_0^I$	$\lambda_0^I$	$h^I$	$\Omega_b^{II} (h^{II})^2 / \Omega_b^I (h^I)^2$
1.0	0.0	0.50	0.022	180	0.38	0.00	0.576	1.98
1.0	0.0	0.50	0.022	120	0.39	0.00	0.574	1.98
1.0	0.0	0.50	0.030	180	0.32	0.00	0.594	2.21
0.6	0.0	0.60	0.040	180	0.29	0.00	0.693	1.55
0.6	0.4	0.60	0.040	180	0.29	0.29	0.694	1.55

The distribution of dark matter particles at present epoch is displayed in Fig. 3 as an example for the model parameter set (1.0, 0.0, 0.5), where the particles in the range  $-3 \text{ Mpc} \leq a_0 x^3 \leq 3 \text{ Mpc}$  are plotted. The corresponding distributions of particles in the  $\bar{x}^k$  coordinates are displayed in Fig. 4. It is found that at the present epoch, the (dark matter) particles in the inner region near the boundary seem to have been mixed with those in the outer region, so that their distributions are quite complicated in the outer region near the boundary.



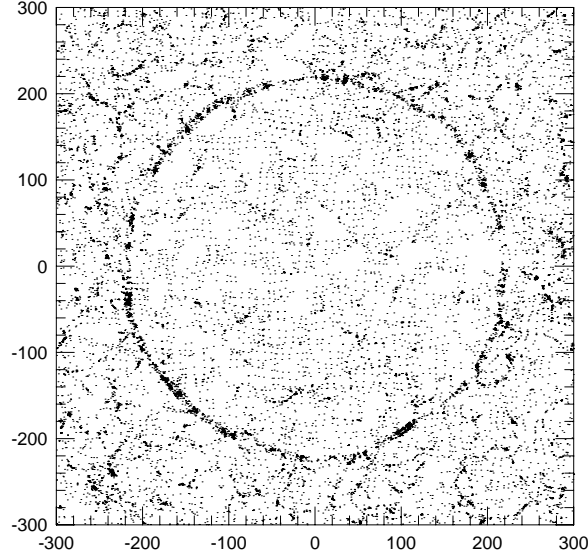


Fig. 3. The distribution of dark matter particles in the  $(a_0 x^1, a_0 x^2)$  plane at the present epoch in the case  $(\Omega_0^{\text{II}}, \lambda_0^{\text{II}}) = (1, 0)$  and  $R_b h = 180$  Mpc. The length of the region displayed is  $600/h$  Mpc, and its width is  $6/h$  Mpc.

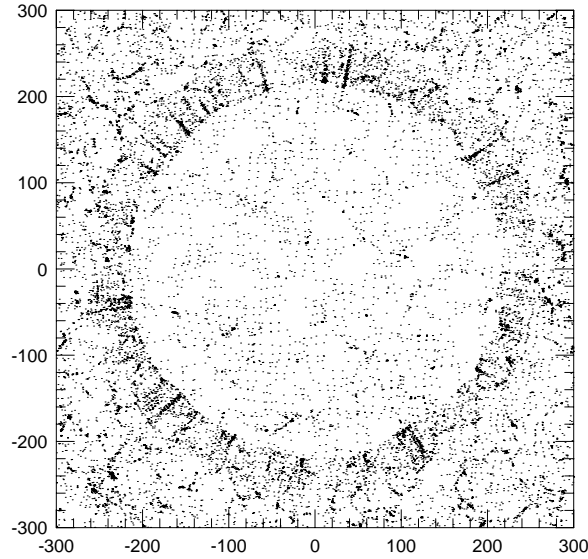


Fig. 4. The distribution of dark matter particles in the  $(a_0 \bar{x}^1, a_0 \bar{x}^2)$  plane at the present epoch in the case  $(\Omega_0^{\text{II}}, \lambda_0^{\text{II}}) = (1, 0)$  and  $R_b h = 180$  Mpc. The length of the region displayed is  $600/h$  Mpc, and its width is  $6/h$  Mpc.

#### §4. Theoretical two-point correlations

In this section the two-point correlations ( $\xi$ ) are derived from the numerical models given in the previous section. Their values in the inner region, with  $r < r_b$ , and the outer region, with  $r_p > r \gg r_{b1}$ , have simple behavior, but they are complicated in the intermediate region,  $r_b < r < r_{b1}$ , because uncorrelated particles are mixed there. Here the correlations ( $\xi_i$  and  $\xi_o$ ) in the inner and outer regions, respectively, were calculated using the particle positions in the average comoving coordinates ( $\bar{x}^k$ ) for various cases with  $R_b h = 180$  Mpc, which were treated in the previous sections. They are assumed to take the form  $\xi = (r_0/R)^\gamma$  with  $\gamma = 1.7$  to derive the correlation lengths  $r_0$ . The results are given in Table II.

Table II. Correlation lengths and ratios of two-point correlations in the two regions of the models with  $R_b h = 180$  Mpc. Here,  $h = h^{\text{II}}$

$\Omega_0^{\text{II}}$	$\lambda_0^{\text{II}}$	$h^{\text{I}}/h^{\text{II}}$	$r_0^{\text{II}}h$	$r_0^{\text{I}}h$	$\xi^{\text{I}}/\xi^{\text{II}}$	$\Omega_0^{\text{II}}h^{\text{II}}/(\Omega_0^{\text{I}}h^{\text{I}})$
1.0	0.0	1.152	5.2	4.2	1.5	2.3
1.0	0.0	1.188	5.6	3.8	2.1	2.6
0.6	0.0	1.155	6.5	5.0	1.6	1.8
0.6	0.4	1.156	5.4	3.9	1.8	1.8

It is found from this result that the ratio  $\xi_o/\xi_i$  is about 2.0 in the case  $\Omega_0^{\text{II}} = 1.0$ ,  $\lambda_0^{\text{II}} = 0.0$ ,  $h^{\text{I}}/h^{\text{II}} = 1.188$ , and in other cases, it is somewhat smaller. Thus the situation in which the ratio of correlations for dark matter particles is larger than 1.5 is common to these models with a local void. Here we compare this ratio with the observed ratio for galaxies. In general this is difficult, because the clustering of galaxies depends not only on the background model, but also on their luminosity through the bias effect. For galaxies with comparatively low luminosity, however, the bias effect on the clustering seems to be small, and the ratio for dark matter may be equal to that for galaxies with  $M_{bJ} = -18 - -21$ . Thus it can be concluded that the theoretical ratio ( $\xi_o/\xi_i$ ) can account for the change in the observed ratio for galaxies over the range  $M_{bJ} = -18 - -21$ .

Now let us consider the power spectra in the two regions. If the spatial scales are much less than  $r_b$  or much larger than  $r_b$ , we can treat the power spectrum in each region as that of a homogeneous model with the fitting formula ( $i = \text{I and II}$ )

$$P_i(k) \propto k \left[ \frac{\ln(1 + 2.34q_i)}{2.34q_i} \right]^2 [1 + 3.89q_i + (16.1q_i)^2 + (5.46q_i)^3 + (6.71q_i)^4]^{-1/2}, \quad (4.1)$$

where  $q_i = k(h^i)^{-1}/\Gamma_i$ , and the shape parameter is  $\Gamma_i \equiv \Omega_0^i h^i \exp[-\Omega_B^i (1 + \sqrt{2h^i/\Omega_0^i})]$ , depending on the baryon density.<sup>42)</sup> In the outer region we can derive  $\Omega_0^{\text{II}}h^{\text{II}}$  from the measurements of CMB anisotropies, but at present we have only the rough value  $\Omega_0^{\text{II}}h^{\text{II}} = 0.3 - 0.5$ , which is obtained as those with weak prior from Boomerang, DASI and MAXIMA experiments.<sup>5), 7), 9)</sup> In the inner region also we can roughly determine  $\Omega_0^{\text{I}}h^{\text{I}}$  from the treatment of Peacock and Dodds,<sup>43)</sup> in which they derived the reconstructed linear data for the density contrasts of galaxies and clusters. Their data for the case  $k/h < 0.02$  Mpc<sup>-1</sup> correspond to our outer region and have comparatively large uncertainty. Therefore, by assigning larger weights to the data for

$k/h > 0.03 \text{ Mpc}^{-1}$ , we estimate  $\Omega_0^I h^I$  as  $\Omega_0^I h^I = 0.2 - 0.25$ . Thus we obtain the observational ratio  $\Omega_0^{II} h^{II} / (\Omega_0^I h^I) = 1.0 - 2.5$  at present.

In our models, by comparison, we have the ratios listed in the last column of Table II in the cases (1), (2) and (3). It is seen that our models correspond to the case with comparatively large ratios.

### §5. Bulk flows in the inner region

If we observe from the center C, the average velocity field would be isotropic, and the directions of the velocities of particles would be radial at each point in the inner region. For an off-center observer O (being a realistic observer), however, the average velocity field is anisotropic, and the non-radial component is found to be significant, when each velocity ( $\vec{v}$ ) in the inner region is divided into the component ( $v_r$ ) in the radial direction  $O \rightarrow A$  and the component ( $v_p$ ) in the direction  $C \rightarrow O$  as

$$\vec{v} = v_r \vec{l} + v_p \vec{n}. \quad (5.1)$$

Here  $\vec{l}$  and  $\vec{n}$  are the unit vectors in the directions of  $O \rightarrow A$  and  $C \rightarrow O$ , respectively (see Fig. 5), and we have

$$v_r = \left[ \vec{v} \vec{l} - (\vec{v} \vec{n})(\vec{l} \vec{n}) \right] / \left[ 1 - (\vec{l} \vec{n})^2 \right] \quad (5.2)$$

and

$$v_p = \left[ \vec{v} \vec{n} - (\vec{v} \vec{l})(\vec{n} \vec{l}) \right] / \left[ 1 - (\vec{l} \vec{n})^2 \right]. \quad (5.3)$$

Then the mean physical value  $V_p$  for  $v_p$  is defined by

$$V_p \equiv a_0 \left( \sum_{i \in I_*} v_{p(i)} \right) / N_*, \quad (5.4)$$

where  $i$  is the particle index and  $N_*$  is the particle number in the set  $I_*$ . This value depends on the model parameters and is proportional to the distance  $R_{co} (\equiv a_0 r_{co})$  from C to O. By choosing O in  $N_0$  different directions with equal  $R_{co}$ , we can derive the  $N_0$  independent values of  $V_p$ . Using them, we obtained an average value of  $V_p$  and the dispersion ( $\sigma_p$ ) for  $N_0 = 6$ . Their values are listed in Table III for models with  $R_b = 180/h \text{ Mpc}$  and  $R_{co} = 50$  or  $60/h \text{ Mpc}$ , where  $h = h^{II}$ . The values for  $V_{\text{bulk}} \equiv (H_0^I - H_0^{II}) R_{co} = 100(h^I - h^{II}) R_{co}$  also are listed, and it is found that  $V_p$  is equal to  $V_{\text{bulk}}$ . In the inner region, the average velocity field of galaxies is equal to that of dark matter, and it therefore appears that this velocity corresponds to the bulk flow of clusters with the velocity  $\sim 700 \text{ km s}^{-1}$ , which was measured by Hudson et al.<sup>11)</sup> and Willick.<sup>12)</sup> If the measured velocity is smaller,  $V_{\text{bulk}}$  can be adjusted to it by taking smaller  $R_{co}$ , because  $V_{\text{bulk}}$  is proportional to  $R_{co}$ .

### §6. Baryon content

Let us now consider the baryon content in our models with a void. Here we assume that all inhomogeneities evolved gravitationally from perturbations with very

Table III. Bulk velocities and their dispersions

$\Omega_0^{\text{II}}$	$\lambda_0^{\text{II}}$	$R_{\text{co}}h$ Mpc	$V_p$ km/s	$\sigma_p$ km/s	$V_{\text{bulk}}$ km/s
1.0	0.0	50	764.5	49.5	760
1.0	0.0	40	752.8	46.6	752
0.6	0.0	50	774.5	66.8	775
0.6	0.4	50	777.6	57.1	780

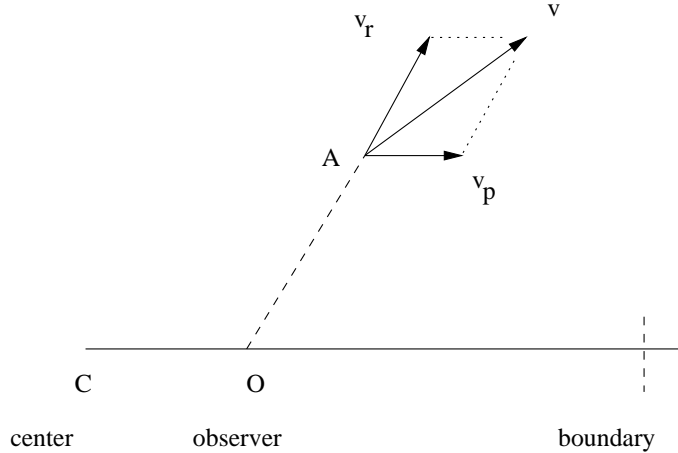


Fig. 5. Velocity vectors in the inner region.

small amplitudes at the stage of nuclear synthesis and that dark matter and baryons are well mixed, so that the ratio of the baryon density to the matter density is equal everywhere. Then in the case  $(\Omega_0^{\text{I}}, \Omega_0^{\text{II}}) = (0.3, 1.0)$  and  $h^{\text{II}} = h^{\text{I}} \times 0.8$  in the inner (I) and outer (II) regions, we have  $\Omega_0^{\text{II}}/\Omega_0^{\text{I}} = 1.0/0.3$ , so that  $\Omega_0^{\text{II}}(h^{\text{II}})^2 = 2.1 \times \Omega_0^{\text{I}}(h^{\text{I}})^2$  and  $\Omega_b^{\text{II}}(h^{\text{II}})^2 = 2.1 \times \Omega_b^{\text{I}}(h^{\text{I}})^2$ . The ratios  $\Omega_b^{\text{II}}(h^{\text{II}})^2/\Omega_b^{\text{I}}(h^{\text{I}})^2$  for the models we used in our simulations are given in the last column of Table I. It is found from this table that in models with  $\Omega_0^{\text{II}} = 1.0$ , the ratio can be about 2, and in models  $\Omega_0^{\text{II}} = 0.6$ , the ratios are somewhat smaller.

From observational studies of light elements, it has been found that in the remote past, we have  $\Omega_b h^2 \cong 0.025$ , which can be derived from the analysis of deuterium abundance in QSOs for  $z \sim 2$ .<sup>48), 49), 50)</sup> Moreover, recent studies of the CMB anisotropy suggest similar baryon content,  $\Omega_b h^2 = 0.02 - 0.03$ .<sup>5), 7)</sup> Using these observational results in the outer region and the above ratios in the two regions, we obtain  $\Omega_b h^2 = 0.010 - 0.015$  in the inner region. As long as they are produced adiabatically, the baryon/photon ratio ( $\eta$ ) is equal and constant ( $\simeq 7 \times 10^{-10}$ ) everywhere, and therefore, at the stage of primordial nucleosynthesis, the photon number densities also were inhomogeneous. At the present stage, however, they have been equalized in both regions owing to the free propagation of photons.

If the so-called *crisis* of big-bang nucleosynthesis<sup>44), 45)</sup> is actual and  $\eta$  is really inhomogeneous (i.e.  $\eta \simeq 3 \times 10^{-10}$  in the inner region) in connection with the primordial abundance of Li<sup>7</sup>,<sup>46), 47)</sup> it may be necessary in order to avoid this *crisis*, to invoke that the void was produced as a special large-scale structure including non-adiabatic perturbations.

### §7. Concluding remarks

In this paper, we first considered galaxy formation in inhomogeneous models with a local void. The observed distribution of galaxies seems to be homogeneous, but we discussed the possibility that this homogeneity may be due to the complicated feedback processes of galaxy formation and evolution in an inhomogeneous distribution of dark matter halos. In order to clarify observationally the existence of the boundary of the void, it is therefore necessary to investigate galactic distributions in greater detail, such as the distribution of active (colliding) galaxies and two-point correlations.

Next, we derived numerical inhomogeneous models consisting of dark-matter particles with a spherical low-density (inner) region and studied the two-point correlations in the inner and outer regions. It was found that they can be made consistent with the redshift dependence of observed correlations of low-luminosity galaxies. Moreover we derived the bulk flow found by an off-center observer, which may correspond to observed large-scale bulk flow. Finally, we studied the baryon content and discussed the possibility of avoiding the *crisis* of light elements.

In previous papers<sup>13), 14), 15)</sup> we calculated the luminosity and angular-diameter distances to derive the  $[m, z]$  relation, and found that the distances in our models with a local void are similar to those in  $\Lambda$ -dominant homogeneous models in the redshift interval  $0 < z < z_m (\approx 1)$ . Thus in the observations using mainly the distances, such as the number-counts of galaxies and clusters, the theoretical relations  $N(m)$  in the above two different types of models are similar in the interval  $0 < z < z_m$ . Even if the observations of  $N(m)$  rule out the SCDM model ( $\Lambda = 0$ ),<sup>51), 52)</sup> our models with a local void and  $\Lambda = 0$  may be consistent with the observations, like the  $\Lambda$ -dominant homogeneous models.

It is well known that we are in the low-density region ( $\Omega_0 \sim 0.3$ ), but the total matter density and baryon content in the remote region ( $z > 1$ ) have not yet been established clearly through observation. From the observations of the CMB anisotropies, we can constrain the model parameters and baryon content. The recent results of Boomerang, DASI and MAXIMA experiments,<sup>5), 7), 9)</sup> however, seem to differ and to be partially inconsistent with respect to the density parameter and the baryon content. Therefore a precise measurement by the MAP satellite is needed to determine these values more accurately. If the additional data from SNIa with  $z > 1.5$  are also obtained from the SNAP satellite and large telescopes, like Subaru etc., the model parameters in the remote region could be determined with much better precision.

### Acknowledgments

The author is grateful to Y. Suto and T. Sugimoto for providing him with their useful tree code for simulations. This work was supported by a Grant-in Aid for Scientific Research (No. 12440063) from the Ministry of Education, Science, Sports and Culture, Japan. He also acknowledges use of the YITP computer system for the numerical analyses.

## References

- [1] B. P. Schmidt, N. B. Suntzeff, M. M. Phillips, R. A. Schommer, A. Clocchiatti, R. P. Kirshner, P. Garnavich, P. Challis et al., *Astrophys. J.* **507** (1998), 46.
- [2] A. G. Riess, A. V. Filippenko, P. Challis, A. Clocchiatti, A. Diercks, P. M. Garnavich, R. L. Gilliland et al., *Astron. J.* **116** (1998), 1009.
- [3] A. G. Riess, A. V. Filippenko, W. Li and B. Schmidt, *Astron. J.* **118** (2000), 2668.
- [4] S. Perlmutter, G. Aldering, G. Goldhaber, R. A. Knop, P. Nugent, D. E. Groom, P. G. Castro, S. Deustua et al., *Astrophys. J.* **517** (1999), 565.
- [5] A. E. Lange et al., *Phys. Rev.* **D63** (2001), 042001.
- [6] A. T. Lee et al., *Astrophys. J.* **561** (2001), L1.
- [7] R. Stomper et al., *Astrophys. J.* **561** (2001), L7.
- [8] N. W. Halverson et al., astro-ph/0104489.
- [9] C. Pryke et al., astro-ph/0104490.
- [10] K. Tomita, *Astrophys. J.* **529** (2000), 26.
- [11] M. J. Hudson, R. J. Smith, J. R. Lucey, D. J. Schlegel and R. L. Davies, *Astrophys. J.* **512** (1999), L79.
- [12] J. A. Willick, *Astrophys. J.* **522** (1999), 647.
- [13] K. Tomita, *Astrophys. J.* **529** (2000), 38.
- [14] K. Tomita, *Mon. Not. R. Astron. Soc.* **326** (2001), 287.
- [15] K. Tomita, *Prog. Theor. Phys.* **106** (2001), 929, astro-ph/0104141.
- [16] A. G. Riess et al., astro-ph/0104455.
- [17] S. D. M. White and M. J. Rees, *Mon. Not. R. Astron. Soc.* **183** (1978), 341.
- [18] S. D. M. White and C. S. Frenk, *Astrophys. J.* **379** (1991), 52.
- [19] G. Kauffmann, B. Guiderdoni and S. D. M. White, *Mon. Not. R. Astron. Soc.* **267** (1994), 981.
- [20] S. Cole, A. Aragon-Salamanca, C. S. Frenk, J. F. Navarro and S. E. Zepf, *Mon. Not. R. Astron. Soc.* **271** (1994), 781.
- [21] S. Cole, C. G. Lacey, C. M. Baugh and C. S. Frenk, *Mon. Not. R. Astron. Soc.* **319** (2000), 168.
- [22] R. S. Somerville and J. R. Primack, *Mon. Not. R. Astron. Soc.* **310** (1999), 1087.
- [23] G. Kauffmann, A. Nusser and M. Steinmetz, *Mon. Not. R. Astron. Soc.* **286** (1997), 795.
- [24] G. Kauffmann, J. M. Colberg, A. Diaferi and S. D. M. White, *Mon. Not. R. Astron. Soc.* **303** (1999), 188.
- [25] A. J. Benson, C. S. Frenk, C. M. Baugh, S. Cole and C. G. Lacey, *Mon. Not. R. Astron. Soc.* **327** (2001), 1041.
- [26] R. S. Somerville et al., *Mon. Not. R. Astron. Soc.* **320** (2001), 289.
- [27] R. Cen and J. Ostriker, *Astrophys. J.* **417** (1993), 404.
- [28] N. Katz, D. H. Weinberg and L. Herquist, *Astrophys. J. Suppl.* **105** (1996), 19.
- [29] C. S. Frenk, A. E. Evrard, S. D. M. White and F. J. Summers, *Astrophys. J.* **472** (1996), 460.
- [30] S. T. Kay, F. R. Pearce, C. S. Frenk and A. Jenkin, *Mon. Not. R. Astron. Soc.* **330** (2002), 113.
- [31] A. A. Thoul and D. H. Weinberg, *Astrophys. J.* **465** (1996), 608.
- [32] G. Efstathiou, *Mon. Not. R. Astron. Soc.* **256** (1992), 43p.
- [33] M. Nagashima, N. Gouda and N. Sugiura, *Mon. Not. R. Astron. Soc.* **305** (1999), 449.
- [34] G. Efstathiou, *Mon. Not. R. Astron. Soc.* **317** (2000), 697.
- [35] C. Marinoni, P. Monaco, G. Giuricin and B. Costantini, *Astrophys. J.* **521** (1999), 50.
- [36] R. O. Marzke, L. N. da Costa, P. S. Pellegrini, C. N. A. Willmer and M. J. Geller, *Astrophys. J.* **503** (1998), 617.
- [37] S. Folkes, S. Ronen, I. Price, O. Lahav, M. Colless, S. Maddox, K. Deeley, K. Glazebrook et al., *Mon. Not. R. Astron. Soc.* **308** (1999), 459.
- [38] E. Zucca, G. Zamorani, G. Vettolani, A. Cappi, R. Merighi, M. Mignoli, H. MacGillivray, C. Collins et al., *Astron. Astrophys.* **326** (1997), 477.
- [39] D. S. Madgwick et al., astro-ph/0107197.
- [40] P. Norberg et al., *Mon. Not. R. Astron. Soc.* **328** (2001), 64.
- [41] I. Zehavi et al., *Astrophys. J.* **571** (2002), 172.
- [42] N. Sugiyama, *Astrophys. J. Suppl.* **100** (1995), 281.
- [43] J. A. Peacock and S. J. Dodds, *Mon. Not. R. Astron. Soc.* **267** (1994), 1020.

- [44] K. A. Olive and D. N. Schramm, *Nature* **360** (1992), 439.
- [45] G. Steigman, *Critical Dialogue in Cosmology* (World Scientific. Publ. Co. Ltd., 1997), p 63.
- [46] K. A. Olive, astro-ph/0009475.
- [47] S. G. Ryan, T. C. Beers, K. A. Olive, B. D. Fields and J. E. Norris, *Astrophys. J.* **530** (2000), L57.
- [48] O'Meara, D. Tytler, D. Kirkman, N. Suzuki, J. X. Prochaska, D. Lubin and A. M. Wolfe, *Astrophys. J.* **552** (2001), 718.
- [49] M. Pettini and D. V. Bowen, *Astrophys. J.* **560** (2001), 41.
- [50] S. Burles, K. M. Nollett and M. S. Turner, *Astrophys. J.* **552** (2001), L1.
- [51] Y. Yoshii and B. A. Peterson, *Astrophys. J.* **444** (1995), 15.
- [52] T. Totani, Y. Yoshii, F. Iwamuro, T. Maihara and K. Motohara, *Astrophys. J.* **550** (2001), L137.